

Magnetic-field-driven topological transitions in non-centrally-symmetric energy spectrum of 2D electron gas with Rashba-Dresselhaus spin-orbit interaction

I.V. Kozlov and Yu.A. Kolesnichenko*

B. Verkin Institute for Low Temperature Physics and Engineering of the National Academy of Sciences of Ukraine, 47 Nauky Ave., Kharkiv 61103, Ukraine

Two dimension electron systems with combined Rashba and Dresselhaus spin orbit interaction (SOI) having a complicated energy spectrum with a conical point and four critical points are promising candidates to observe electron topological transitions. In the present paper we have investigated the evolution of the electron spectrum and isoenergetic contours under the influence of parallel magnetic field. General formulas for energies of critical points for arbitrary values of SOI constants and magnetic field are found. The existence of critical magnetic fields at which a number of critical points is changed has been predicted. The magnetic field driving topological Lifshitz transitions in the geometry of isoenergetic contours have been studied. Van Hove's singularities in the electron density of states are calculated. The obtained results can be used for theoretical investigations of different electron characteristics of such 2D systems.

PACS numbers: 64.70.Tg, 73.20.At, 71.70.Ej

I. INTRODUCTION

In the fundamental paper [1] Ilya M. Lifshitz predicted "electron transitions" - abrupt changes of the Fermi surface topology under continuous variation of some parameter: pressure, chemical potential etc. These transitions result in anomalies in different kinetic and thermodynamic characteristics of metals that stipulated special attention to their detailed investigations (see [2–4] for review). In recent years the interest in Lifshitz transitions get renewed in view of intensive studies of new electron systems: graphene, topological insulators, semimetals, superconductors, Dirac semimetals, and Weyl semimetals, in which different types of electron topological transitions take place [5]. Low dimensional systems with spin - orbit interaction (SOI) [6, 7] are possible candidates to observe topological transitions in the energy spectrum as well. Manifestations of topological transitions in a magnetic susceptibility of 3D semiconductors with SOI had been predicted by Boiko and Rashba [8]. Recently the enhanced orbital paramagnetism related to the topological transition was observed in a layered semiconductor BiTeI when the Fermi energy E_F is near the crossing point of the Rashba spin-split conduction bands [9]

Among a variety of spin - orbit materials the two dimensional (2D) systems made of zincblende III-V, wurtzite, SiGe semiconductors, semiconductor quantum wells, etc., occupy a special place possessing combined Rashba - Dresselhaus (R-D) SOI [10–13] (see [14] for review). Interplay between two types of SOI results in anisotropic spin - split Fermi contours which leads to an anisotropic magnetoresistance [15], an enhancement of electron propagation along a narrow range of real-space angles from an isotropic source [17], anisotropic Friedel oscillations [18, 19] and so on.

In the presence of SOI a parallel magnetic field \mathbf{B} results not only in the appearance of a Zeeman energy but also it affects the dispersion law of charge carriers [20], changing the geometry and breaking, the central symmetry of 2D Fermi contours [21]. It is a possible way to manipulate with anisotropy of transport characteristics that seems to be promising for practical applications. The energy spectrum of 2D electrons with R-D SOI in the in-plane magnetic field \mathbf{B} can be easily obtained, but to date the information on the evolution of energy branches with the changes of direction and absolute value of vector \mathbf{B} is incomplete and disconnected [22–24]. In the recent paper [25] an electronic transport in 2D electron gas subjected to the in-plane magnetic field for the case of Rashba SOI had been studied theoretically. Singularities of a conductivity and a spin polarization as functions of the Fermi level or magnetic field, which occurs when the Fermi level passes through the Van Hove singularity [26], were analyzed. It was predicted that the transport anisotropy dramatically changes near the singularity. Such anisotropy was reported in an experiment [27].

In this paper we present a consistent consideration of changes in the energy spectrum of 2D electrons with R-D SOI under the variations of the parallel magnetic field. Special attention will be paid to the magnetic-field-induced 2D electron topological transitions. The structure of the paper is as follows. Section II contains some known information which is the basis of subsequent investigations. We present the Hamiltonian of the system, its eigenvalues and eigenfunctions. The energy spectrum in the absence of the magnetic field is discussed from the point of view of possibilities of topological transitions. In Sec. III the evolution of energy spectrum for arbitrary value and direction of vector \mathbf{B} is studied. We predict the existence of critical fields B_{c1} and B_{c2} at which the number of critical points (minima and saddle points) of the energy surfaces is changed. So a possibility to create artificial degenerate critical points of energy spectrum ap-

* kolesnichenko@ilt.kharkov.ua

pears. Limiting cases of weak and strong magnetic field are considered. In Sec. IV, as examples, we present explicit analytical results for the energies of critical points, their position in the \mathbf{k} - space, and critical values B_{c1} and B_{c2} for the magnetic field directed along the symmetry axes. Variations of topology of isoenergetic contours, which are 2D analogue of Fermi surface, under variations of the magnetic field have been analyzed in Sec. V. In Sec. VI the singular part of the electron density of states is discussed. The obtained formulas allow to determine SOI constants from van Hove singularities [26]. We conclude the paper with some final remarks and a summary of main results in Sec.VII.

II. HAMILTONIAN OF THE SYSTEM. ENERGY SPECTRUM AT ZERO MAGNETIC FIELD

Our calculations are based on the widely used model of the 2D single-electron Hamiltonian taking into account linear terms of R-D SOI (see, for example, [17, 18, 22, 23, 30–32])

$$\hat{H}_0 = \frac{\hat{\mathbf{P}}^2}{2m}\sigma_0 + \frac{\alpha}{m}(\sigma_x\hat{P}_y - \sigma_y\hat{P}_x) + \frac{\beta}{\hbar}(\sigma_x\hat{P}_x - \sigma_y\hat{P}_y) - \frac{g^*}{2}\mu_B\mathbf{B}\sigma. \quad (1)$$

Here $\hat{\mathbf{P}} = \hat{\mathbf{p}} + e\mathbf{A}/c$ is the operator of the generalized momentum, $\hat{\mathbf{p}} = \hbar\hat{\mathbf{k}} = -i\hbar\nabla = (\hat{p}_x, \hat{p}_y)$ is the operator of the in-plane momentum, \mathbf{A} is the vector potential of the in-plane magnetic field $\mathbf{B} = (B_x, B_y, 0)$, m is an effective electron mass, $\sigma_{x,y,z}$ are Pauli matrices, $\sigma = (\sigma_x, \sigma_y, \sigma_z)$ is the Pauli vector, $\hat{\sigma}_0$ is unit matrix 2×2 , α and β are Rashba (α) [33] and Dresselhaus [34] (β) constants of SOI, μ_B is the Bohr magneton, and g^* is an effective g-factor of the 2D system. For definiteness we assume α, β to be nonnegative values and $\alpha \geq \beta$.

In the framework of 2D model the Hamiltonian (1) does not depend on a component $P_z = p_z + eA_z/c$ of the generalized momentum and in the Coulomb gauge, $\mathbf{A} = (0, 0, B_x y - B_y x)$, $\nabla \cdot \mathbf{A} = 0$, can be rewritten as

$$\hat{H}_0 = \frac{\hbar^2 (\hat{k}_x^2 + \hat{k}_y^2)}{2m}\sigma_0 + \alpha(\sigma_x\hat{k}_y - \sigma_y\hat{k}_x) + \beta(\sigma_x\hat{k}_x - \sigma_y\hat{k}_y) - \frac{g^*}{2}\mu_B(B_x\sigma_x + B_y\sigma_y). \quad (2)$$

where $\hat{\mathbf{k}}$ is the wave vector operator. Neglecting by cubic terms in the Dresselhaus part of Eqs. (1), (2) we assume a narrow quantum well and small 2D wave vectors k of electrons in a conduction band, $k \ll \pi/w$, where w is the well width.

The eigenvalues and the eigenfunctions of the Hamil-

tonian (2) are (see, for example, [22])

$$\epsilon_{1,2}(\mathbf{k}) = \frac{\hbar^2 k^2}{2m} \pm \sqrt{(h_x + \alpha k_y + \beta k_x)^2 + (h_y - \alpha k_x - \beta k_y)^2}, \quad (3)$$

$$h_{x,y} = -\frac{g^*}{2}\mu_B B_{x,y},$$

$$\psi_{1,2}(\mathbf{r}) = \frac{1}{2\pi\sqrt{2}}e^{i\mathbf{k}\mathbf{r}} \begin{pmatrix} 1 \\ \pm e^{i\theta} \end{pmatrix}. \quad (4)$$

The angle θ defines an average spin direction for two branches of energy spectrum (3), $\theta = \theta_2 = \theta_1 + \pi$,

$$\tan \theta = \frac{h_y - \alpha k_x - \beta k_y}{h_x + \alpha k_y + \beta k_x}, \quad (5)$$

which depends on the wave vector and the magnetic field.

In the absence of magnetic field $h_x = h_y = 0$ the energy spectrum (3) is centrosymmetric $\epsilon_{1,2}(\mathbf{k}) = \epsilon_{1,2}(-\mathbf{k})$, and has two symmetry axes $k_x = k_y$ and $k_x = -k_y$. At $\alpha \neq \beta$ energy branches $\epsilon = \epsilon_1(\mathbf{k})$ and $\epsilon = \epsilon_2(\mathbf{k})$ (energies as the function of the wave vector are three dimension surfaces in ϵ, k_x, k_y space) touch each other at the single point $\mathbf{k} = 0$, which is a conical (Dirac) point. In this point the energy of ϵ_1 branch has a smallest value $\epsilon_1(0) = 0$. The energy branch $\epsilon = \epsilon_1(\mathbf{k}) \geq 0$ as the function of wave vector components k_x, k_y is a convex surface for any values of parameters. The energy surface corresponding to the second branch $\epsilon = \epsilon_2(\mathbf{k})$ has two degenerate minima $\epsilon_2^{\min 1,2} = -\frac{m}{2\hbar^2}(\alpha + \beta)^2$ in the points $k_x^{\min 1,2} = k_y^{\min 1,2} = \mp \frac{m}{\sqrt{2}\hbar^2}(\alpha + \beta)$, two saddle points $k_x^{sad 1,2} = -k_y^{sad 1,2} = \pm \frac{m}{\sqrt{2}\hbar^2}(\alpha - \beta)$ corresponding to the energy $\epsilon_2^{sad 1,2} = -\frac{m}{2\hbar^2}(\alpha - \beta)^2$, and the conical point $\epsilon_2(0) = 0$ at $\mathbf{k} = 0$.

The isoenergetic contours of constant energy $\epsilon_{1,2}(\mathbf{k}) = E$ (2D contours of a constant energy $\epsilon = E$ in the k_x, k_y plane) are a 2D analogue of 3D Fermi surface pockets. At positive energies $E > 0$ the spectrum has two spin - split contours (see Fig. 1b). The larger contour (1 (ϵ_2), 2 (ϵ_2) in Fig. 1b) belongs to the branch $\epsilon = \epsilon_2$. The smaller contour (1 (ϵ_1), 2 (ϵ_1) in Fig. 1b) of the branch $\epsilon = \epsilon_1$ is always situated inside the larger one. For $\epsilon_2(\mathbf{k}) = E < 0$ the isoenergetic contour become not simply connected: In the range $\epsilon_2^{sad 1,2} < E < 0$ inside the larger isoenergetic contour the contour of smaller radius is situated (contour 4 in the insert in Fig. 1a). The electron velocity on this contour is directed along an inner normal, i.e. this contour can be interpreted as a "hole" one. At $E = \epsilon_2^{sad 1,2}$ the contours becomes self-crossed. In the range $\epsilon_2^{\min 1,2} < E < \epsilon_2^{sad 1,2}$ this contour splits into two parts which do not span the point $\mathbf{k} = 0$. The contours of the branch $\epsilon = \epsilon_2(\mathbf{k})$ is non-convex in the energy interval

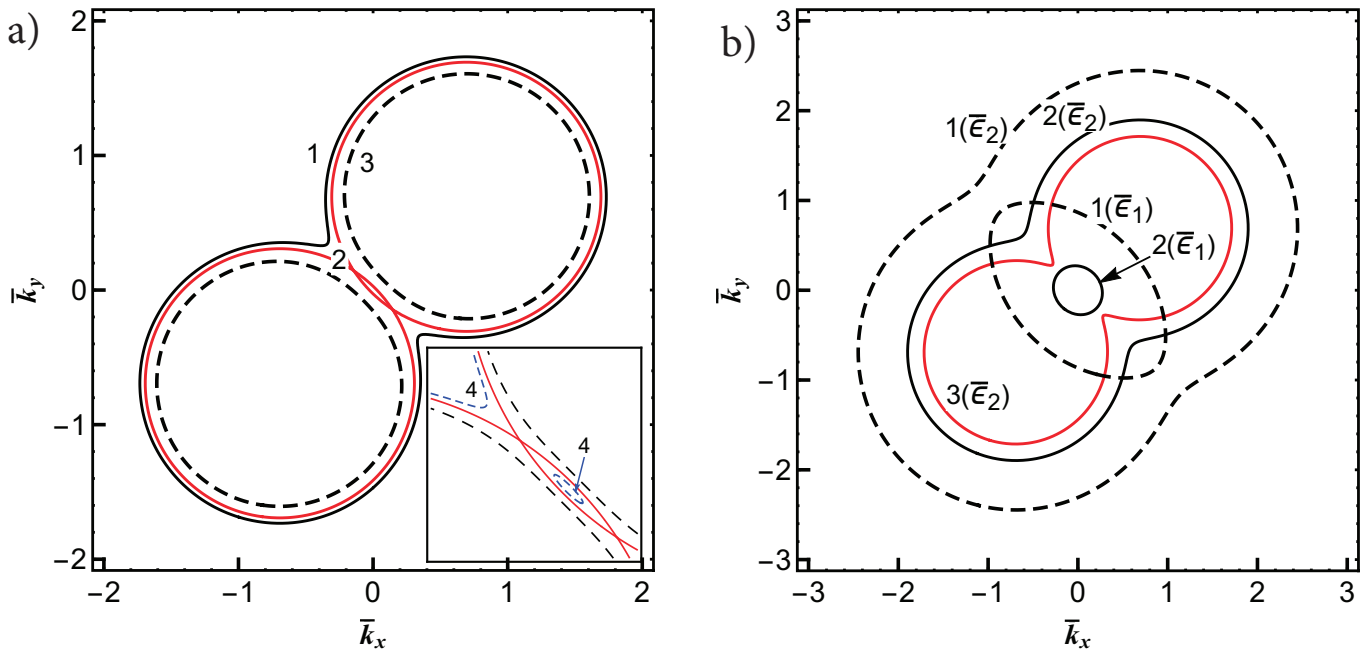


FIG. 1. Isoenergetic contours for different energies E at $\hbar = 0$, $\epsilon_2^{\min 1,2} = -0.72$, $\bar{\epsilon}_2^{sad1,2} = -0.02$, $\bar{\alpha} = 0.6$, $\bar{\beta} = 0.4$. a) The contours belong to the branch $\epsilon = \epsilon_2$ at $E \leq 0$: $E = 0$, black solid contour (1); $\bar{E} = \bar{\epsilon}_2^{sad1,2} = -0.02$, red self-crossed contour (2); $\bar{E} = -0.1$, dashed contour (3). In the insert: $\bar{E} = -0.01$, blue short-dashed contour (4). b) The contours $\epsilon_{1,2} = E$ at $E > 0$; $\bar{E} = 1$, dashed contours (1); $\bar{E} = 0.2$, black solid contours (2); $E = 0$, red solid contour (3).

[19]

$$\epsilon_2^{sad1,2} \leq E < -\frac{m(\alpha + \beta)^2 (\alpha^2 - 6\alpha\beta + \beta^2)}{2\hbar^2(\alpha - \beta)^2}. \quad (6)$$

In the special case, $\alpha = \beta$, two energy spectrum branches contact along the parabola $\epsilon_1 = \epsilon_2 = \frac{\hbar^2 k^2}{2m}$ in the plane crossing the symmetry axis $k_x = -k_y$.

Plotting different dependencies in this paper we use for numerical computations the dimensionless values

$$\begin{aligned} \bar{\alpha} &= \frac{m\alpha}{\hbar^2 k_0}, & \bar{\beta} &= \frac{m\beta}{\hbar^2 k_0}, & \bar{h} &= \frac{h}{\epsilon_0}, \\ \bar{k} &= \frac{k}{k_0}, & \bar{\epsilon} &= \frac{\epsilon}{\epsilon_0}, & k_0 &= \sqrt{2m\epsilon_0/\hbar}, \end{aligned} \quad (7)$$

where $\epsilon_0 > 0$ is a constant of energy dimension, for example, an absolute value of Fermi energy.

Figure 1 demonstrates the full set of Lifshitz transitions under changes of the energy: the appearance (or disappearance) of the new detached region at $E = 0$ (Fig. 1b), disruption (or formation) of the contour "neck" (Fig. 1a) and the appearance of the critical self-crossing contour at $\epsilon_2^{sad1,2} = E$ (contour 2 in Fig. 1a).

The concentration of 2D electron gas created in heterostructures, and hence the Fermi energy, can be controlled by means of a gate electrode. Why a magnetic field is needed? In the system with spin - orbit interaction an electric field perpendicular to the plane of 2D electrons not only shifts the Fermi level but also changes the

Rashba SOI constant [35–37]. That may make the interpretation of experimental results ambiguous. The parallel magnetic field plays the role of independent parameter which can tune critical points of the energy spectrum to the Fermi energy. In the next sections we consider possibilities to drive by characteristics of energy spectrum of 2D electron gas with R-D SOI by means of in-plane magnetic field.

III. ARBITRARY MAGNETIC FIELD DIRECTION. GENERAL RELATIONS

In the parallel magnetic field and $\alpha \neq \beta$ the point of energy branch contact moves from the point $\mathbf{k} = 0$ to the point $\mathbf{k} = \mathbf{k}_0$ whose coordinates of which must be found from the condition

$$\sqrt{(h_x + \alpha k_{y0} + \beta k_{x0})^2 + (h_y - \alpha k_{x0} - \beta k_{y0})^2} = 0. \quad (8)$$

It is easy to see that Eq. (8) is equivalent to the system of linear inhomogeneous equations

$$\alpha k_{y0} + \beta k_{x0} = -h_x; \quad \alpha k_{x0} + \beta k_{y0} = h_y, \quad (9)$$

and we have

$$\begin{aligned} k_{x0} &= h \frac{\alpha \sin \varphi_h + \beta \cos \varphi_h}{\alpha^2 - \beta^2}, \\ k_{y0} &= -h \frac{\alpha \cos \varphi_h + \beta \sin \varphi_h}{\alpha^2 - \beta^2}, \end{aligned} \quad (10)$$

where angle φ_h defines the magnetic field direction $\mathbf{h} = h(\cos \varphi_h, \sin \varphi_h, 0)$. The energy value corresponding to the point $\mathbf{k} = \mathbf{k}_0 = (k_{x0}, k_{y0})$ (10) is given by

$$\epsilon_1(\mathbf{k}_0) = \epsilon_2(\mathbf{k}_0) = E_0 = \hbar^2 \hbar^2 \frac{\alpha^2 + \beta^2 + 2\alpha\beta \sin 2\varphi_h}{2m(\alpha^2 - \beta^2)^2}. \quad (11)$$

If the SOI constants are equal, $\alpha = \beta$, the equations (9) have nonzero solutions only if $h_x = -h_y$. In this case the branches contact along the parabola

$$\begin{aligned} \epsilon_{cont}(k_{y1}, h) &= \frac{\hbar^2 k_{y1}^2}{2m} + \frac{\hbar^2 h^2}{8m\alpha^2}, \\ k_{x1} &= \frac{k_x + k_y}{\sqrt{2}} = \frac{h}{2\alpha}, \quad k_{y1} = \frac{k_x - k_y}{\sqrt{2}}. \end{aligned} \quad (12)$$

For any other directions of the vector \mathbf{h} the branches do not have common points for $\alpha = \beta$.

For further analysis of the energy spectrum at $\alpha \neq \beta$ it is useful to introduce polar coordinates $\tilde{k} > 0$, and f with the center in the point \mathbf{k}_0 (10):

$$k_x = k_{x0} + \tilde{k} \cos f, \quad k_y = k_{y0} + \tilde{k} \sin f. \quad (13)$$

Note that new coordinates only shift the energy spectrum in \mathbf{k} -space and they don't change differential characteristics of $\epsilon = \epsilon_{1,2}(\mathbf{k})$ surfaces.

In coordinates \tilde{k}, f (13) the energies $\epsilon_{1,2}$ take the simple form

$$\epsilon_{1,2}(\tilde{k}, f) = \frac{\hbar^2 \tilde{k}^2}{2m} - \frac{\hbar^2 \tilde{k}}{m} \lambda_{1,2}(f) + E_0, \quad (14)$$

where

$$\begin{aligned} \lambda^{(1,2)}(f) &= h \frac{\alpha \sin(f - \varphi_h) - \beta \cos(f + \varphi_h)}{\alpha^2 - \beta^2} \\ &\mp \frac{m}{\hbar^2} \sqrt{\alpha^2 + \beta^2 + 2\alpha\beta \sin(2f)}, \end{aligned} \quad (15)$$

$$\lambda^{(2)}(f) = -\lambda^{(1)}(f + \pi). \quad (16)$$

Substituting Eqs. (13) into formula (5) one finds that spin directions are antisymmetric, $\theta(f + \pi) = \theta(f) + \pi$, with respect to the point $\mathbf{k}_0 = (k_{x0}, k_{y0})$.

The sign of the Gauss curvature $K^{(1,2)}(\tilde{k}, f)$ of energy surfaces $\epsilon = \epsilon_{1,2}(\tilde{k}, f)$ is defined by the sign of the determinant $\det(H)$ of the Hessian matrix

$$H = \begin{pmatrix} \frac{\partial^2 \epsilon_{1,2}}{\partial k_x^2} & \frac{\partial^2 \epsilon_{1,2}}{\partial k_x \partial k_y} \\ \frac{\partial^2 \epsilon_{1,2}}{\partial k_y \partial k_x} & \frac{\partial^2 \epsilon_{1,2}}{\partial k_y^2} \end{pmatrix}. \quad (17)$$

In coordinates (13) one finds

$$\det(H) = \frac{\hbar^4}{m^2 \tilde{k}} \left[\tilde{k} - \ddot{\lambda}^{(1,2)}(f) - \lambda^{(1,2)}(f) \right]. \quad (18)$$

Here and in all formulas below the points above functions denote the derivative with respect to the angle f . From Eq. (15) one can see that the sum of $\lambda^{(1,2)}$ and its second derivatives $\ddot{\lambda}^{(1,2)}$ do not depend on magnetic field and has the definite sign

$$\ddot{\lambda}^{(1,2)}(f) + \lambda^{(1,2)}(f) = \mp \frac{m}{\hbar^2} \frac{(\alpha^2 - \beta^2)^2}{(a^2 + 2\alpha\beta \sin(2f) + \beta^2)^{3/2}}. \quad (19)$$

From Eqs. (18), (19) it follows that $K^{(1)}(\tilde{k}, f) > 0$ for any values of parameters, i.e. the surface $\epsilon = \epsilon_1(\tilde{k}, f)$ is the convex one.

Critical points (\tilde{k}_ν, f_ν) of the energy spectrum should be found from the system of equations

$$\frac{\partial \epsilon_{1,2}}{\partial \tilde{k}} = \frac{\hbar^2}{m} \left(\tilde{k} - \lambda^{(1,2)}(f) \right) = 0, \quad \tilde{k} \geq 0, \quad (20)$$

$$\frac{\partial \epsilon_{1,2}}{\partial f} = -\frac{\hbar^2}{m} \tilde{k} \dot{\lambda}^{(1,2)}(f) = 0, \quad (21)$$

from which we give

$$\tilde{k}_\nu^{(1,2)} = \lambda^{(1,2)}(f_\nu^{(1,2)}) \quad (a), \quad \dot{\lambda}^{(1,2)}(f_\nu^{(1,2)}) = 0 \quad (b); \quad (22)$$

where index ν numerates the roots of Eq.(21). According to the definition the variable \tilde{k} is an absolute value of electron wave vector in coordinates (13). Only solutions for which $\tilde{k}_\nu^{(1,2)} = \lambda^{(1,2)}(f_\nu^{(1,2)}) > 0$ have the physical meaning.

The obvious equality Eq.(16) gives the relations between solutions (22):

$$\begin{aligned} f_\nu^{(1)} &= f_\nu^{(2)} + \pi, \quad \tilde{k}(f_\nu^{(1)}) = -\tilde{k}(f_\nu^{(2)}), \\ \dot{\lambda}^{(1)}(f_\nu^{(1)}) &= -\dot{\lambda}^{(2)}(f_\nu^{(2)}). \end{aligned} \quad (23)$$

The determinant $\det(H)$ (18) in critical points reads

$$\det(H(\tilde{k}_\nu, f_\nu)) = -\frac{\hbar^4}{m^2 \tilde{k}} \ddot{\lambda}^{(1,2)}(f) \Big|_{\tilde{k}=\tilde{k}_\nu, f=f_\nu^{(1,2)}}, \quad \tilde{k} > 0. \quad (24)$$

If $\ddot{\lambda}^{(1,2)} \neq 0$, the critical point is nondegenerate. From Eq. (24) we conclude that the negative second derivative $\ddot{\lambda}^{(1,2)}(f_\nu^{(1,2)}) < 0$ corresponds to energy minima $\epsilon_{1,2}(\tilde{k}_\nu, f_\nu^{(1,2)}) = \epsilon_{1,2}^{\min}$ and for saddle points of non-convex surface $\epsilon_2(\tilde{k}_\nu, f_\nu^{(1,2)}) = \epsilon_2^{\text{sad}}$ the second derivative is positive $\ddot{\lambda}^{(2)}(f_\nu^{(1,2)}) > 0$. As it easy to see from the Eqs. (14),(22) the energies in critical points are written as

$$\epsilon_{1,2}^{\text{crit}} = \epsilon_{1,2}(\tilde{k}_\nu, f_\nu^{(1,2)}) = E_0 - \frac{\hbar^2}{2m} \left(\lambda^{(1,2)}(f_\nu^{(1,2)}) \right)^2, \quad (25)$$

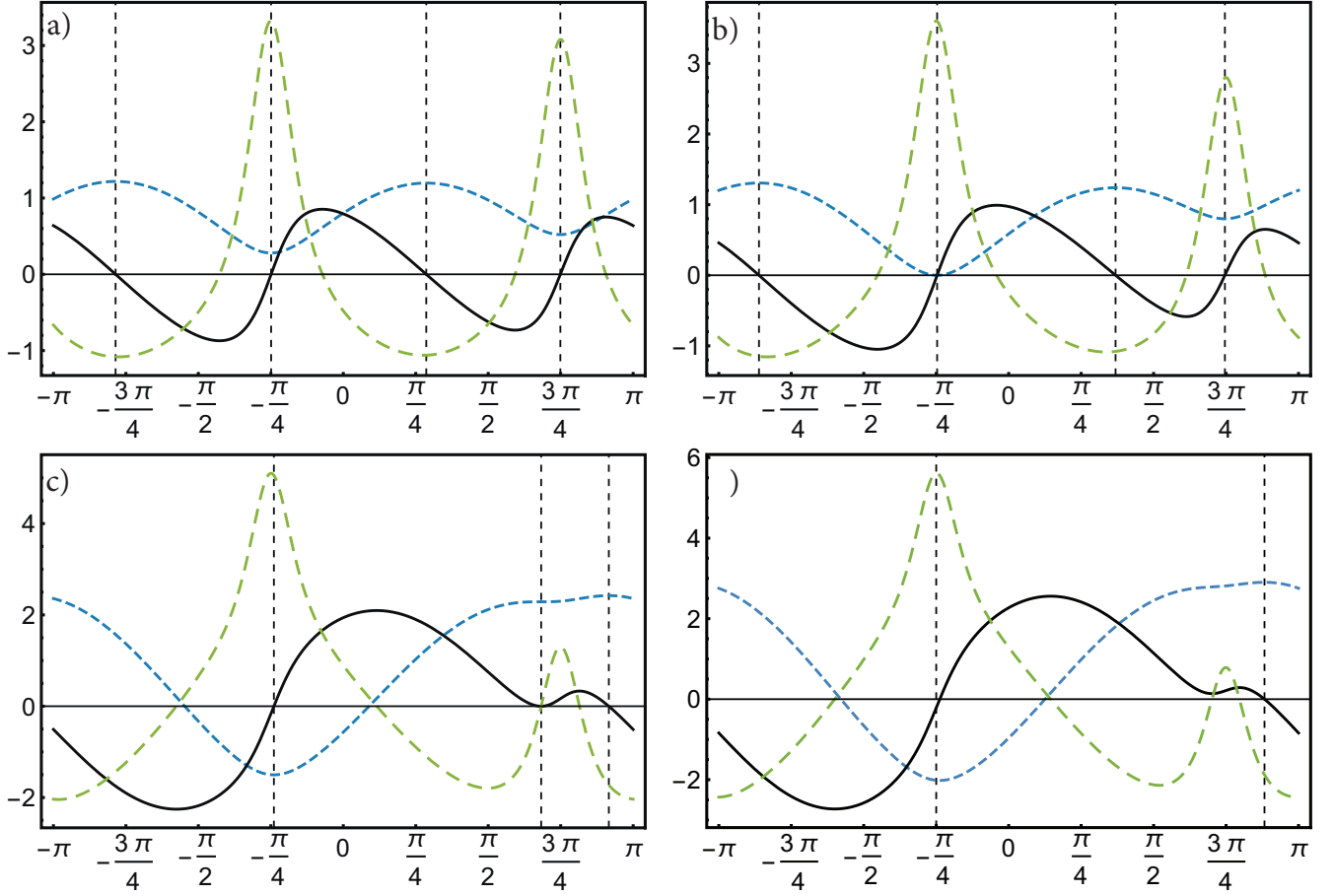


FIG. 2. The dependencies of the function $\lambda_2(f)$ (15) (short dashed lines), its first $\dot{\lambda}_2(f)$ (solid lines) and second $\ddot{\lambda}_2(f)$ (long dashed lines) derivatives on the angle $f \in [-\pi, \pi]$ for different values of magnetic field h : a) $\bar{h} = 0.05 < \bar{h}_{c2} = 0.1655$; b) $h = h_{c2}$; c) $\bar{h} = \bar{h}_{c1} = 0.7867$; d) $\bar{h} = 1 > \bar{h}_{c1}$. Vertical dashed lines show angles $f = f_{\nu}^{(2)}$ corresponding $\dot{\lambda}_2(f_{\nu}^{(2)}) = 0$. For SOI constants and magnetic field direction we used the values $\bar{\alpha} = 0.8$, $\bar{\beta} = 0.4$, $\varphi_h = \pi/3$.

i.e. all critical points are situated below energy level $E = E_0$. So, the evolution of either energy branch of 2D electrons with R-D SOI under influence of parallel magnetic field is completely described by means of the single function $\lambda^{(1,2)}(f)$ (15).

For arbitrary magnetic field the equation (22b) can be transformed to quartic equation for $\cos(2f_{\nu}^{(1,2)})$, the exact solutions of which are well known. Unfortunately they are so lengthy that not suitable to any analytical calculation. Nevertheless for numerical computations the solution of equation (22b) presents no problems.

The limiting cases of weak and strong magnetic fields can be analyzed by means of expansions of exact eigenenergies (3). For the weak magnetic field the power expansion of energy ϵ_2 (3) on h gives energies of critical points and their positions. As a results of direct calculations one obtains the following expressions for two minima

$$\epsilon_2^{\min 1,2} \simeq -\frac{m}{2\hbar^2}(\alpha + \beta)^2 \mp h \sin\left(\varphi_h - \frac{\pi}{4}\right),$$

$$h \ll \frac{m}{\hbar^2}(\alpha + \beta)^2, \quad (26)$$

$$k_x^{\min 1,2} = k_y^{\min 1,2} \simeq \mp \frac{m}{\hbar^2} \frac{\alpha + \beta}{\sqrt{2}} - \frac{(\alpha - \beta)h \sin\left(\varphi_h + \frac{\pi}{4}\right)}{\sqrt{2}(\alpha + \beta)^2}, \quad (27)$$

and two saddle points

$$\epsilon_2^{\text{sad}1,2} \simeq -\frac{m}{2\hbar^2}(\alpha - \beta)^2 \pm h \sin\left(\varphi_h + \frac{\pi}{4}\right),$$

$$h \ll \frac{m}{\hbar^2}(\alpha - \beta)^2, \quad (28)$$

$$k_x^{\text{sad}1,2} = -k_y^{\text{sad}1,2} \simeq \pm \frac{\alpha - \beta}{\sqrt{2}} \frac{m}{\hbar^2} - \frac{h(\alpha + \beta) \sin\left(\varphi_h - \frac{\pi}{4}\right)}{\sqrt{2}(\alpha - \beta)^2}. \quad (29)$$

The branch ϵ_1 in this case hasn't extremum. The energy ϵ_1 reaches the least value $\epsilon_1(\mathbf{k}_0) = E_0$ (11) in the point of branch contact $\mathbf{k}_0 = (k_{x0}, k_{y0})$ (10).

In the strong magnetic field $h \gg \frac{m}{\hbar^2}(\alpha^2 + \beta^2 - 2\alpha\beta \sin 2\varphi_h)$ the power series of $\epsilon_{1,2}$ (3) on $1/h$ gives the energy minima $\epsilon_{1,2}^{\min}$ of both branches

$$\epsilon_{1,2}^{\min} \simeq \pm h - \frac{m}{2\hbar^2}(\alpha^2 + \beta^2 - 2\alpha\beta \sin 2\varphi_h), \quad (30)$$

$$\begin{aligned} k_{x1,2}^{\min} &\simeq \pm \frac{m}{\hbar^2} (\alpha \sin \varphi_h - \beta \cos \varphi_h), \\ k_{y1,2}^{\min} &\simeq \pm \frac{m}{\hbar^2} (\beta \sin \varphi_h - \alpha \cos \varphi_h). \end{aligned} \quad (31)$$

So, with the increasing of the magnetic field the energy spectrum evolves from the energy branch ϵ_2 having four critical points and the branch ϵ_1 without critical points to the spectrum every branch of which has single critical (minimum) point. How such evolution occurs? For arbitrary magnetic field direction some general conclusions can be made of the basis of the properties of functions $\lambda^{(1,2)}(f)$ (15) and its derivatives $\lambda^{(1,2)}(f)$, $\ddot{\lambda}^{(1,2)}(f)$.

As it has been concluded above the branch $\epsilon = \epsilon_1$ is convex and hasn't saddle points. It is clear from Eq. (15) at weak magnetic field ($h \rightarrow 0$) $\lambda^{(1)}(f) < 0$ for any angle f , i.e. for energy branch $\epsilon = \epsilon_1(\mathbf{k})$ the Eq. (20) hasn't positive solutions $\tilde{k} > 0$. The critical value $h = h_{c2}$ can be derived by means of the equation $\lambda^{(1)}(h = h_{c2}; f) = 0$ from which we find

$$h_{c2} = \frac{(\alpha^2 - \beta^2)^2}{\sqrt{\alpha^4 + 6\alpha^2\beta^2 + \beta^4 + 4\alpha\beta(\alpha^2 + \beta^2)\sin 2\varphi_h}}. \quad (32)$$

Substituting $\lambda^{(1)}(f)$ (15) in Eq. (25) and taking into account the positiveness of the function $\lambda^{(1)}(f_{\nu}^{(1)}) > 0$ at $h > h_{c2}$, it is easy to show that $0 \leq \epsilon_1^{\min} \leq E_0$ for any values of parameters. As it follows from Eq. (23) the appearance of minima of the branch ϵ_1 is accompanied by the disappearance of saddle point of the branch ϵ_2 .

The energy surface $\epsilon = \epsilon_2$ has regions of negative Gauss curvature. The derivative $\lambda^{(2)}(f)$ is the sum the oscillatory functions with periods 2π and π . Depending on the magnetic field value it has two zeros at $h > h_{c1}$ and four zeros at $h < h_{c1}$ in the range $[-\pi, \pi]$. Numbers of zeros $\lambda^{(2)}(f)$ having different sign of second derivative $\ddot{\lambda}^{(2)}(f)$ are equal. The critical value h_{c1} can be found from the condition of the coalescence of two zeros of $\lambda^{(2)}(h, f)$ with different signs of second derivative $\ddot{\lambda}^{(2)}(h; f)$ which in this point vanishes, i.e. one should search two unknown quantities h_{c1} , f_c from two equations

$$\dot{\lambda}^{(2)}(h_{c1}, f_c) = 0; \quad \ddot{\lambda}^{(2)}(h_{c1}, f_c) = 0. \quad (33)$$

We couldn't find the analytical solution of this system for arbitrary magnetic field orientation. The critical fields h_{c1} in an explicit form for special directions of vector \mathbf{h} are found in the next section. Note that the sign of the difference $h_{c2} - h_{c1}$ is not fixed for given α , β and depends on the magnetic field direction.

The evolution of the branch $\epsilon = \epsilon_2(\mathbf{k})$ can be understood from Fig. 2. In the magnetic field $h < \min(h_{c1}, h_{c2})$, $\tilde{k}_{\nu}^{(2)} = \lambda^{(2)}(f_{\nu}^{(2)}) > 0$, and there are four critical points $\dot{\lambda}^{(2)}(f_{\nu}^{(2)}) = 0$ - two minima $\epsilon_2^{\min 1,2}(\ddot{\lambda}^{(1,2)}(f_{\nu}) < 0)$ and two saddle points $\epsilon_2^{\text{sad}1,2}(\ddot{\lambda}^{(1,2)}(f_{\nu}) > 0)$ (Fig. 2a). At $h = h_{c2}$ one of the saddle points coincides with the point of branch contact,

$\tilde{k}_{\nu}^{(2)} = \lambda^{(2)}(f_{\nu}^{(2)}) = 0$, and "disappear" (Fig.2b). In the magnetic field $h = h_{c1}$ the minimum and saddle points of energy surface $\epsilon = \epsilon_2$ "annihilate" (Fig.2c) and in larger fields $h > \max(h_{c1}, h_{c2})$ the branch $\epsilon = \epsilon_2(\mathbf{k})$ has one absolute minimum (Fig. 2d).

In next paragraph we consider some cases when exact formulas become an elementary and give clear illustrations of general conclusion of this paragraph.

IV. MAGNETIC FIELD ALONG SYMMETRY AXIS

For the direction of the magnetic field along one of the symmetry axis the energy spectrum preserves the symmetry with respect to other axis. This circumstance essentially simplify the solution of equations obtained above.

a) Magnetic field directed along $k_x = -k_y$ axis

Let us consider the magnetic field direction $\varphi_h = 3\pi/4$. In this case the equation (21), from which the angles f_{ν} ($\nu = 1, 2, 3, 4$) corresponding to zeros of derivative $\lambda_{1,2}$ can be found. The Eq. (22b) has four solutions in the interval $[-\pi, \pi]$. Two solutions do not depend on magnetic field and SOI constants

$$f_1^{(1,2)} = -\frac{3\pi}{4}, \quad f_2^{(1,2)} = \frac{\pi}{4}, \quad (34)$$

and two solutions exist in the finite interval of value $h \in [0, h_{c1}]$

$$\begin{aligned} f_3^{(1,2)}(h) &= -\frac{\pi}{4} \mp \arcsin(\eta), \\ f_4^{(1,2)}(h) &= \frac{3\pi}{4} \pm \arcsin(\eta), \end{aligned} \quad (35)$$

where

$$\begin{aligned} \eta(\alpha, \beta, h) &= \frac{h(\alpha - \beta)}{2\sqrt{\alpha\beta(h_{c1}h_{c2} - h^2)}}, \\ \eta \leq 1 &\Leftrightarrow h \leq h_{c1}. \end{aligned} \quad (36)$$

The functions $\lambda^{(2)}(f_{\nu}^{(1,2)})$ and $\ddot{\lambda}^{(2)}(f_{\nu}^{(1,2)})$ which define the energy of critical points and their character are presented in Appendix. The critical magnetic fields in the case under consideration are

$$h_{c1} = \frac{4m}{\hbar^2}\alpha\beta; \quad h_{c2} = \frac{m}{\hbar^2}(\alpha + \beta)^2. \quad (37)$$

In accordance with Eqs. (25),(A.1) for any value of magnetic field the energy of the branch $\epsilon = \epsilon_2$ has the minimum $\epsilon_2^{\min 1}$

$$\begin{aligned} \epsilon_2^{\min 1}(h) &= \epsilon^{\text{crit}1}(h), \quad f_1^{(2)} = -\frac{3\pi}{4}; \\ \tilde{k}_1^{(2)}(h) &= \frac{m}{\hbar^2}(\alpha + \beta) + \frac{h}{\alpha + \beta}. \end{aligned} \quad (38)$$

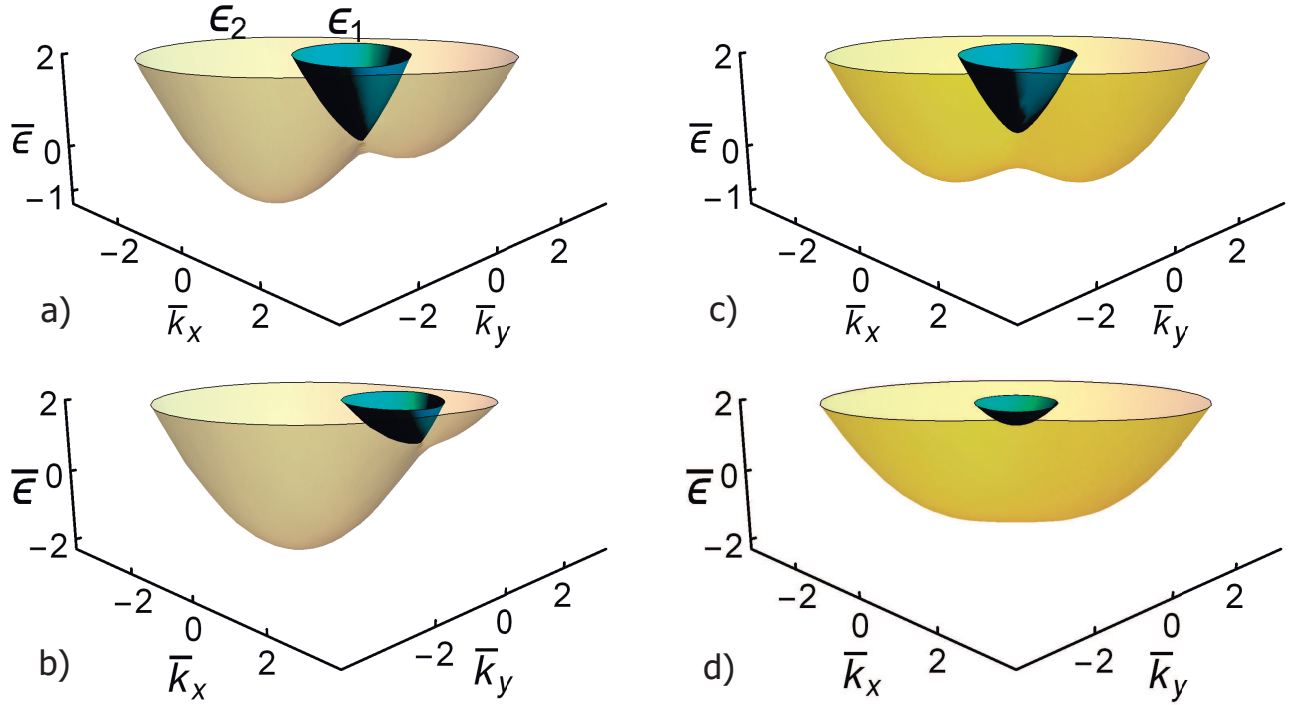


FIG. 3. Energy spectrum (3) for the magnetic field directed along $k_x = -k_y$ axis, $\varphi_h = 3\pi/4$, (a,b) and along $k_x = k_y$ axis, $\varphi_h = \pi/4$, (c,d). a,c) $\bar{h} = 0.5 < \bar{h}_{c1} = 1.28, \bar{h}_{c2} = 1.44$; b,d) $\bar{h} = 1.5 > \bar{h}_{c1}, \bar{h}_{c2}$. For SOI constants we used the values $\bar{\alpha} = 0.8, \bar{\beta} = 0.4$.

With an increase in magnetic field the minimum $\epsilon_2^{\min 1}$ moves down. The second minimum of this branch $\epsilon_2^{\min 2}$

$$\begin{aligned} \epsilon_2^{\min 2}(h) &= \epsilon^{\text{crit}2}(h); & f_2^{(2)} &= \frac{\pi}{4}, \\ \tilde{k}_2^{(2)}(h) &= \frac{m}{\hbar^2}(\alpha + \beta) - \frac{h}{\alpha + \beta}, \end{aligned} \quad (39)$$

exists in the field interval $0 \leq h < h_{c1}$. In this interval the branch ϵ_2 has two saddle points with equal energies

$$\begin{aligned} \epsilon_2^{\text{sad}3,4}(h) &= \epsilon^{\text{crit}3,4}(h), & f &= f_{3,4}^{(2)}, \\ \tilde{k}_{3,4}^{(2)}(h) &= \frac{m}{\hbar^2}(\alpha - \beta) \sqrt{1 - \frac{h^2}{h_{c1}h_{c2}}}. \end{aligned} \quad (40)$$

In the field $h \rightarrow h_{c1}$ the minimum $\epsilon_2^{\min 2}$ transforms to the saddle point $\epsilon_2^{\min 2} \rightarrow \epsilon_2^{\text{sad}} = \epsilon^{\text{crit}2}$ (the second derivative $\ddot{\lambda}^{(2)}$ (A.4) changes the sign at $h = h_{c1}$) which blends with two saddle points $\epsilon_2^{\text{sad}3,4}$ (40), i.e. the critical point becomes degenerate

$$\begin{aligned} \epsilon^{\min 2}(h_{c1}) &= \epsilon_2^{\text{sad}}(h_{c1}) = \epsilon_2^{\text{sad}3,4}(h_{c1}) \\ &= -\frac{m}{2\hbar^2}(\alpha^2 - 6\alpha\beta + \beta^2)^2, \\ \tilde{k}_2^{(2)}(h_{c1}) &= \tilde{k}_{3,4}^{(2)}(h_{c1}) = \frac{m(\alpha - \beta)^2}{\hbar^2(\alpha + \beta)}, \\ f_2^{(2)}(h_{c1}) &= f_{3,4}^{(2)}(h_{c1}) = \frac{\pi}{4}. \end{aligned} \quad (41)$$

In larger fields $h_{c1} < h < h_{c2}$ the saddle point ϵ_2^{sad} exists. At $h \rightarrow h_{c2}$ its energy $\epsilon_2^{\text{sad}} \rightarrow E_0$ and this saddle point disappears in the field $h = h_{c2}$ ($\lambda^{(2)}$ (A.1) becomes negative at $h > h_{c2}$)

$$\begin{aligned} \epsilon^{\text{crit}2}(h_{c2}) &= \epsilon_2^{\text{sad}}(h_{c2}) = E_0(h_{c2}) \\ &= \frac{m}{2\hbar^2}(\alpha + \beta)^2, \\ \tilde{k}_2^{(2)}(h_{c2}) &= 0; & f_2^{(2)} &= \frac{\pi}{4}. \end{aligned} \quad (42)$$

In the magnetic fields $h > h_{c2}$ the function $\lambda^{(1)}$ ($\pi/4$) (A.1) becomes positive and first energy branch ϵ_1 acquires the critical point (minimum) $\epsilon_1^{\min} = \epsilon^{\text{crit}2}$

$$\begin{aligned} \epsilon_1^{\min}(h) &= \epsilon^{\text{crit}2}, & f_2^{(1)} &= \frac{\pi}{4}, \\ \tilde{k}_2^{(1)} &= -\frac{m}{\hbar^2}(\alpha + \beta) + \frac{h}{\alpha + \beta}. \end{aligned} \quad (43)$$

The minimum ϵ_1^{\min} moves up with increase in the magnetic field. The discussed evolution of energy spectrum is illustrated in Fig. 3.

b) Magnetic field directed along $k_x = k_y$ axis

In this case the solutions of the Eq. (22b) take the form (we choose $\varphi_h = \pi/4$)

$$\begin{aligned} f_1^{(1,2)} &= \frac{3\pi}{4}, & f_2^{(1,2)} &= -\frac{\pi}{4}, & f_3^{(1,2)}(h) &= \frac{\pi}{4} \mp \arcsin(\eta), \\ f_4^{(1,2)}(h) &= \frac{5\pi}{4} \pm \arcsin(\eta), \end{aligned} \quad (44)$$

where

$$\eta(\alpha, \beta, h) = \frac{h(\alpha + \beta)}{2\sqrt{\alpha\beta(h_{c1}h_{c2} + h^2)}},$$

$$\eta \leq 1 \Leftrightarrow h \leq h_{c1}. \quad (45)$$

The critical magnetic fields are

$$h_{c1} = \frac{4m}{\hbar^2}\alpha\beta, \quad h_{c2} = \frac{m}{\hbar^2}(\alpha - \beta)^2. \quad (46)$$

As it follows from formulas (A.9)-(A.14) in Appendix, at $h < h_{c2}$ the branch $\epsilon = \epsilon_2$ has two minima $\epsilon_2^{\min 1,2}$ with equal energies

$$\epsilon_2^{\min 1,2}(h) = -\frac{m}{2\hbar^2}(\alpha + \beta)^2 - \frac{h^2\hbar^2}{8m\alpha\beta}, \quad h \leq h_{c1},$$

$$k_{3,4}^{(2)} = \frac{m}{\hbar^2}(\alpha + \beta)\sqrt{1 + \frac{h^2}{h_{c1}h_{c2}}}; \quad f = f_{3,4}^{(2)}, \quad (47)$$

and two saddle points $\epsilon_2^{\text{sad}1,2}$ (see Fig. 3a)

$$\epsilon_2^{\text{sad}1,2}(h) = -\frac{m}{2\hbar^2}(\alpha - \beta)^2 \mp h,$$

$$\tilde{k}_{1,2}^{(2)}(f_{1,2}^{(2)}) = \frac{m}{\hbar^2}(\alpha - \beta) \mp \frac{h}{\alpha - \beta},$$

$$f_1^{(2)} = -\frac{\pi}{4}, \quad f_2^{(2)} = \frac{3\pi}{4}. \quad (48)$$

In magnetic field $h = h_{c1}$ the both minima $\epsilon_2^{\min 1,2}$ and the saddle point $\epsilon_2^{\text{sad}1}$ transform into one degenerate critical point

$$\epsilon_2^{\min 1,2}(h_{c1}) = \epsilon_2^{\text{sad}2}(h_{c1}) = -\frac{m}{2\hbar^2}(\alpha^2 + 6\alpha\beta + \beta^2), \quad (49)$$

$$f_3^{(4)}(h_{c1}) = f_4^{(2)}(h_{c1}) = f_2^{(2)} = \frac{3\pi}{4}, \quad (50)$$

$$\tilde{k}_2^{(2)}(h_{c1}) = \tilde{k}_{3,4}^{(2)}(h_{c1}) = \frac{m}{\hbar^2}\frac{(\alpha + \beta)^2}{\alpha - \beta};$$

$$\ddot{\lambda}^{(2)}\left(h_{c1}, \frac{3\pi}{4}\right) = \ddot{\lambda}^{(2)}\left(h_{c1}, f_{3,4}^{(2)}\right) = 0, \quad (51)$$

and for larger fields $h > h_{c1}$ one minimum

$$\epsilon_2^{\min}(h) = -\frac{m}{2\hbar^2}(\alpha - \beta)^2 - h,$$

$$\tilde{k}_1^{(2)}(f_1^{(2)}) = \frac{m}{\hbar^2}(\alpha - \beta) - \frac{h}{\alpha - \beta}, \quad f_1^{(2)} = -\frac{\pi}{4}, \quad (52)$$

and one saddle point remains

$$\epsilon_2^{\text{sad}}(h) = -\frac{m}{2\hbar^2}(\alpha - \beta)^2 + h,$$

$$\tilde{k}_2^{(2)}(f_2^{(2)}) = \frac{m}{\hbar^2}(\alpha - \beta) + \frac{h}{\alpha - \beta}, \quad f_2^{(2)} = \frac{3\pi}{4}, \quad (53)$$

which exists till $h < h_{c2}$.

The first branch $\epsilon = \epsilon_1$ reaches the smallest value

$$E_0 = \frac{h^2\hbar^2}{2m(\alpha - \beta)^2}, \quad (54)$$

at the weak magnetic field $h < h_{c2}$. If $h > h_{c2}$, this branch has the minimum (see Fig. 3b)

$$\epsilon_1^{\min}(h) = -\frac{m}{2\hbar^2}(\alpha - \beta)^2 + h, \quad (55)$$

$$\tilde{k}_1^{(1)} = -\frac{m}{\hbar^2}(\alpha - \beta) + \frac{h}{\alpha - \beta}, \quad f_1^{(1)} = \frac{3\pi}{4}. \quad (56)$$

The results of this paragraph and Fig.3 illustrate a quite different evolution of energy spectrum for the same values of SOI constants but different magnetic field directions.

V. ISOENERGETIC CONTOURS

The dispersion relation of 2D electron gas can be characterized by isoenergetic contours $\epsilon_{1,2} = E = \text{const}$. According to the theory of electron topological transitions [2, 3] when the energy level E crosses the energy of the critical point $\epsilon_{1,2}^{\text{crit}}$ isoenergetic contours change their topology. By analogy with 3D case we name 2D contours at $E = \epsilon_{1,2}^{\text{crit}}$ as critical contours. The critical contours always have the point (\tilde{k}_ν, f_ν) (22) in which the electron velocity $\mathbf{v} = \frac{\partial \epsilon_{1,2}}{\hbar \partial \mathbf{k}} = 0$,

$$|\mathbf{v}| = \sqrt{\left(\frac{\partial \epsilon_{1,2}}{\hbar \partial k_x}\right)^2 + \left(\frac{\partial \epsilon_{1,2}}{\hbar \partial k_y}\right)^2}$$

$$= \frac{\hbar}{m} \sqrt{\left[\left(\tilde{k} - \lambda^{(1,2)}(f)\right)^2 + \left(\dot{\lambda}^{(1,2)}(f)\right)^2\right]}. \quad (57)$$

In this regard a self-crossing contour is not a critical one because $\mathbf{v} \neq 0$ at the cross point. However, one should remember that the cross point is a particular point in a vicinity of which the electron dispersion is linear in the wave vector components. For the minimum point $\epsilon_{1,2}^{\text{crit}} = \epsilon_{1,2}^{\min}$ the contour is absent for energy $E < \epsilon_{1,2}^{\min}$, while for saddle points $\epsilon_{1,2}^{\text{crit}} = \epsilon_{1,2}^{\text{sad}}$ contours exist both at $E < \epsilon_{1,2}^{\text{sad}}$ and $E > \epsilon_{1,2}^{\text{sad}}$.

The positive roots of the equation (see Eq.(14))

$$\epsilon_{1,2}(\tilde{k}, f) = \frac{\hbar^2 \tilde{k}^2}{2m} - \frac{\hbar^2 \tilde{k}}{m} \lambda_{1,2}(f) + E_0 = E \quad (58)$$

describe the isoenergetic contours $k = k_\pm^{(j)}(E, f)$ corresponding to physical electron states in the \mathbf{k} -space for given energy E

$$k_\pm^{(1,2)} = \lambda^{(1,2)} \pm \sqrt{\xi^{(1,2)}}, \quad (59)$$

$$\xi^{(1,2)} = \left(\lambda^{(1,2)}\right)^2 + \frac{2m(E - E_0)}{\hbar^2} \geq 0. \quad (60)$$

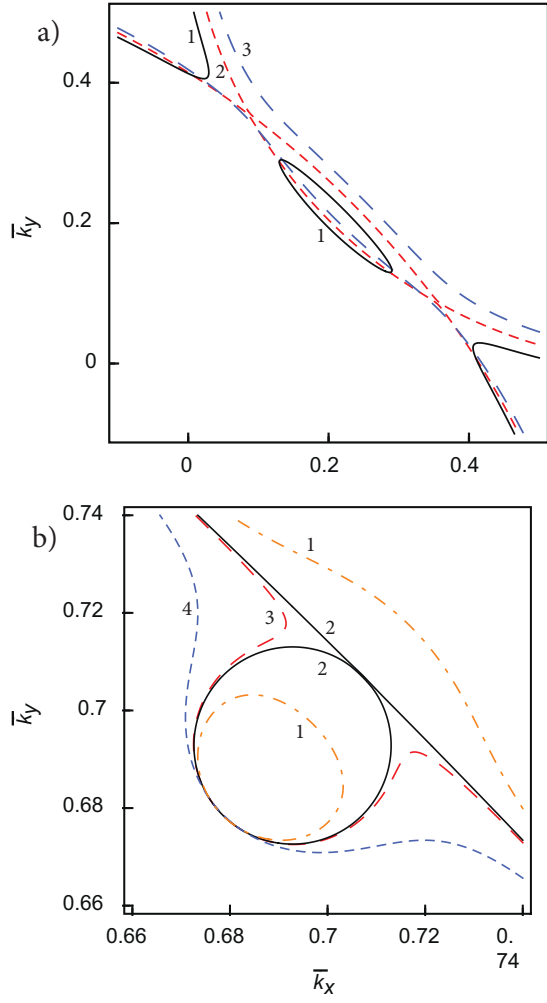


FIG. 4. Fine structure of isoenergetic contours of the branch $\epsilon = \epsilon_2$ for different magnetic fields $\bar{h} \leq \bar{h}_{c1} = 0.96 < \bar{h}_{c2} = 1$. a) The energy $E \leq E_0$ equals to the energy of the saddle point $\bar{E} = \bar{\epsilon}_2^{sad3,4}$ ($\bar{h} = 0.3$) = 0.026875 (40): $\bar{h} = 0.29$, black solid line (1); $\bar{h} = 0.3$, red short-dashed line (2); $\bar{h} = 0.31$, blue long-dashed line (3). b) The energy $\bar{E} < E_0$ (h_{c1}) = 0.4608 equals the energy of the saddle point $\bar{E} = \bar{\epsilon}_2^{sad3,4}$ (\bar{h}_{c1}) = 0.4600 (40) at the critical field $\bar{h}_{c1} = 0.96$: $\bar{h} = 0.9599$, orange dot-dashed line (1); $\bar{h} = \bar{h}_{c1} = 0.96$, black solid line (2); $\bar{h} = 0.96001$, red long-dashed line (3); $\bar{h} = 0.9602$, blue short-dashed line (4). For SOI constants and magnetic field direction we used the values $\bar{\alpha} = 0.8$, $\bar{\beta} = 0.4$, $\varphi_h = 3\pi/4$.

If $E > E_0$, the roots $k_+^{(1,2)} > 0$ for any values of f , while roots $k_-^{(1,2)} < 0$, i.e. there are two contours belonging to different energy branches. For $E < E_0$ real roots of equation (58) exist, if the inequality $2m(E_0 - E)/\hbar^2 \leq (\lambda^{(1,2)})^2$ holds. Roots $k_{\pm}^{(1,2)}$ take positive values for the angles f at which $\lambda^{(1,2)} > 0$. This means that the wave vector crosses the isoenergetic contour twice.

In accordance with Vieta's formulas the roots of Eq.

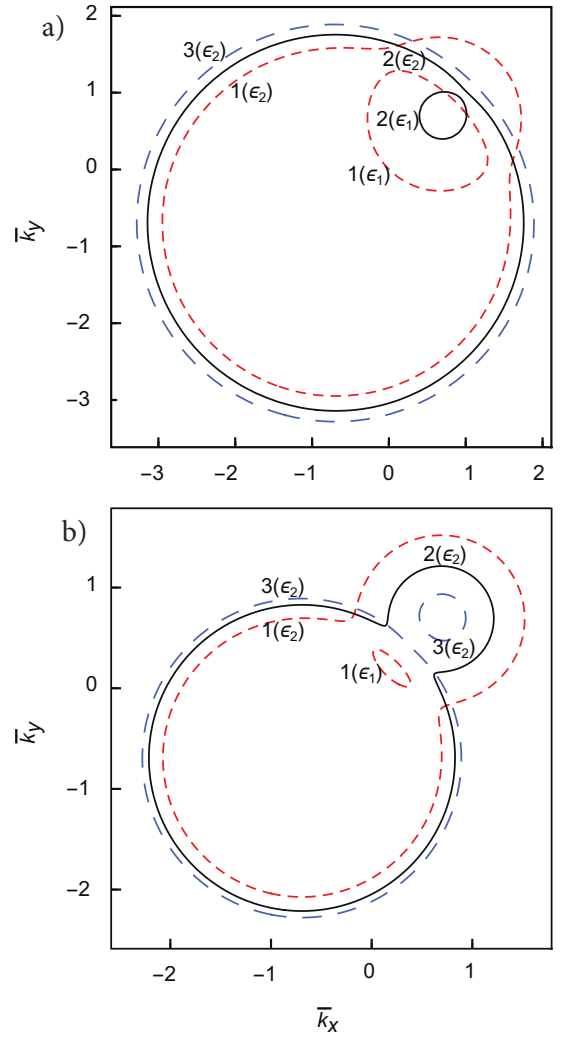


FIG. 5. a) Isoenergetic contours for both branches (labelled in brackets) at the magnetic fields $\bar{h} \geq \bar{h}_{c2} = 1$ and $\bar{E} = 1$: $\bar{h} = \bar{h}_{c2}$, $\bar{E}_0 = 0.5$, $\bar{E} > \bar{\epsilon}_1^{\min} = 0.5$, red short-dashed contours (1); $\bar{h} = 1.45$, $\bar{E}_0 = 1.05$, $\bar{E} > \bar{\epsilon}_1^{\min} = 0.95$, solid contours (2); $\bar{h} = 1.8$, $\bar{E}_0 = 1.62$, $\bar{E} < \bar{\epsilon}_1^{\min} = 1.3$, blue long-dashed contours (3). b) Isoenergetic contours for $\bar{\epsilon}_{1,2} = \bar{E} = \bar{E}_0$ ($\bar{h} = 0.5$) = 0.125, $\bar{h} < \bar{h}_{c1} = 0.96$, $\bar{h}_{c2} = 1$: $\bar{h} = 0.3$, $\bar{E}_0 = 0.045 < \bar{E}$, red short-dashed contours (1); $\bar{h} = 0.5$, $\bar{E}_0 = 0.125 = \bar{E}$, solid contour (2); $\bar{h} = 0.6$, $\bar{E}_0 = 0.18 > \bar{E}$, blue long-dashed contours (3). For SOI constants and magnetic field direction we used the values $\bar{\alpha} = 0.8$, $\bar{\beta} = 0.4$, $\varphi_h = 3\pi/4$.

(58) obey the relations

$$\begin{aligned} k_+^{(1,2)} k_-^{(1,2)} &= \frac{2m(E_0 - E)}{\hbar^2}, \\ k_+^{(1,2)} + k_-^{(1,2)} &= 2\lambda^{(1,2)}, \end{aligned} \quad (61)$$

from which an interesting observation follows: at $E = E_0$ the extremal radii of the contours $k_+^{(1,2)} = 2\lambda^{(1,2)}$, for which $\lambda^{(1,2)} = 0$, give energies (25) and positions (22) of critical points on total surfaces $\epsilon = \epsilon_{1,2}$.

From the properties of energy spectrum which have

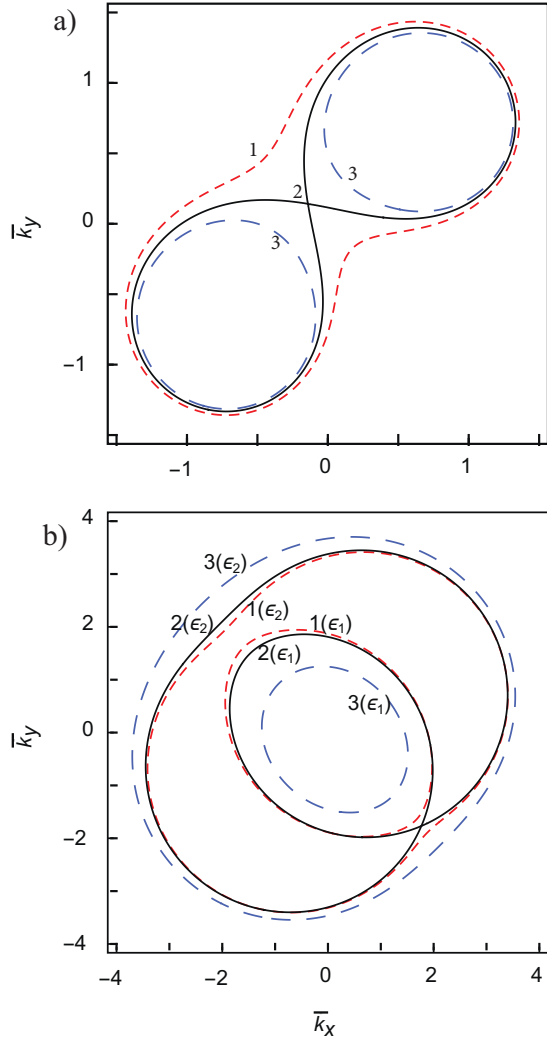


FIG. 6. a) Isoenergetic contours for the energy $\bar{E} = \bar{\epsilon}_2^{sad} (\bar{h} = 0.3) = 0.28$ (53) and $\bar{h}_{c2} = 0.04 < \bar{h} < \bar{h}_{c1} = 0.96$: $\bar{h} = 0.4$, red short-dashed contour(1); $\bar{h} = 0.3$, black solid contour (2); $\bar{h} = 0.2$, blue long-dashed contours (3). b) Isoenergetic contours for both branches (labelled in brackets) at the energy $\bar{E} = \bar{E}_0 (\bar{h} = 0.5) = 3.125$: $\bar{h} = 0.1$, red short-dashed contours (1); $\bar{h} = 0.5$, black solid contour; $\bar{h} = 2$, blue long-dashed contours (3). For SOI constants and magnetic field direction we used the values $\bar{\alpha} = 0.8, \bar{\beta} = 0.4, \varphi_h = \pi/4$.

been discussed in Sec. III some general conclusions related to isoenergetic contours follow: 1) There are no more when two separate contours for given energy E . 2) The contours belonging to the branch $\epsilon = \epsilon_1$ exist for the energies $E > E_0$ at $h < h_{c2}$ and $E > \epsilon_1^{\min}$ at $h > h_{c2}$. Contours $k = k_{\pm}^{(1)}$ (f) are convex by virtue of the equality (19). 3) In magnetic fields $h > h_{c1}$ the contour on the surface $\epsilon = \epsilon_2$ splits into two separated contours for $E < \min(\epsilon_2^{sad1,2})$.

At fixed energy E magnetic field moves the energy of branch contact E_0 (11) and energies of critical points (25) resulting in Lifshitz electron transition of both types -

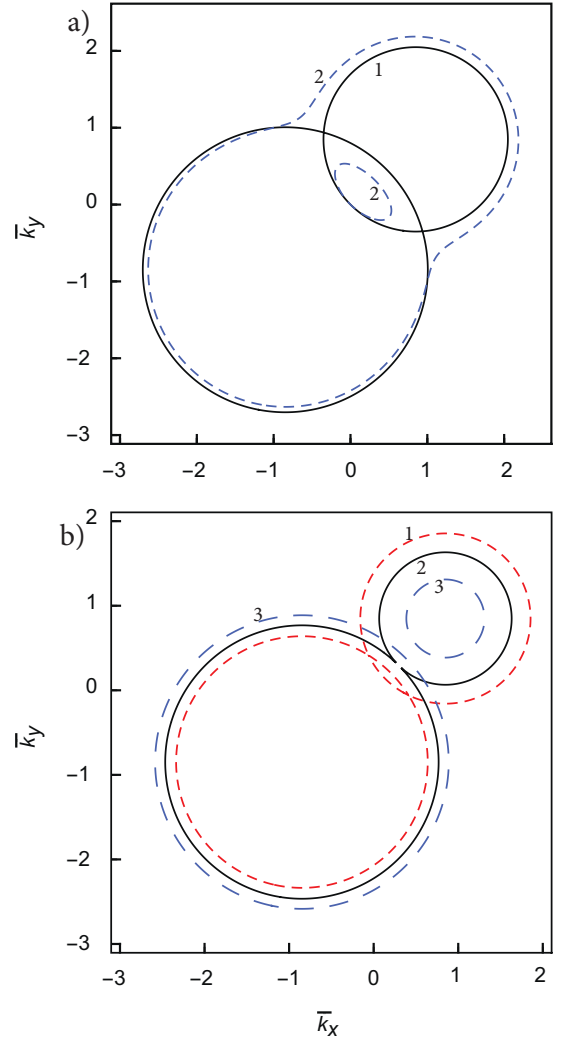


FIG. 7. a) Isoenergetic contours at $\alpha = \beta, \bar{h} = 0.5, \bar{E} = 0.5$ for different magnetic field directions: $\varphi_h = 3\pi/4$, solid contour (1); $\varphi_h = \pi$, blue dashed contours (2). b) Isoenergetic contours at and for the energy corresponding to the minimum of the parabola (11) $\bar{\epsilon}_{cont}^{\min} = \bar{E} = 0.0868$: $\bar{h} = 0.3$, red short-dashed contour (1); $\bar{h} = 0.5$, solid contour (2); $\bar{h} = 0.7$, blue long-dashed contours (3). For SOI constants we used the value $\bar{\alpha} = \bar{\beta} = 0.6$.

appearance of new contour under crossing the energy E by minimum $\epsilon_{1,2}^{\min}$ and disruption of the "neck" at $E = \epsilon_2^{sad}$.

At equal SOI constants $\alpha = \beta$ and magnetic field direction along the axis $k_x = -k_y$ for energies $E > \hbar^2 h^2 / 8m\alpha^2$ isoenergetic contours have two common contact points. Either contour consists of two arcs of the radius (see Fig. 7),

$$k^{(\pm)} = \sqrt{\frac{2m}{\hbar^2} \left(E + \frac{2m\alpha^2}{\hbar^2} \mp h \right)}. \quad (62)$$

Spin directions on each arc composing united contour are opposite, $\theta_+ = 3\pi/4$ or $\theta_- = -\pi/4$, and arcs, which have

the same spin direction θ_{\pm} form total circumference.

Figures 4 and 5 illustrate some of the explicit results obtained in Sec. IVa for the magnetic field directed along the axis $k_x = -k_y$. Figure 4a shows the changes in the fine structure of isoenergetic contours of the branch $\epsilon = \epsilon_2$ for the energy close to the energy of saddle point $\epsilon_2^{sad3,4}(h)$ (40) at the magnetic fields far from the critical values $h < h_{c1}, h_{c2}$ (37). In this case we observe a specific topological transition of the contour splitting in the transverse to the "neck" direction. With the increase in the magnetic field the electron and "hole" contours (curves 1) form unified critical contour with two crossing points (curve 2). The critical contour breaks at the crossing points in the transverse direction forming two electron contours (curves 3). Figure 4b shows the disruption of the "neck" in the case when the energy $E < E_0(h_{c1})$ equals the energy of the saddle point $E = \epsilon_2^{sad3,4}(h_{c1})$ (40) at the critical field h_{c1} (37). Two separate contours (curves 1) touch at $h = h_{c1}$ and in a higher field form a single non-convex contour (curves 3,4).

Figure 5 illustrates another type of the topological transition in the magnetic field: disappearance (or appearance) of a new detached region. Isoenergetic contours for both branches at the magnetic fields $h \geq h_{c2}$ are shown. With an increase in the magnetic field the minimum $\epsilon_1^{\min}(h)$ of the branch $\epsilon = \epsilon_1$ moves up (curves 1 and 2) and at $E = \epsilon_1^{\min}(h)$ crosses the energy level. At this field the contour related to the branch $\epsilon = \epsilon_1$ disappears (curve 3). In Fig. 6b we show the similar topological transition at $h < h_{c2}$ when E_0 is the smallest value of the branch $\epsilon = \epsilon_1$. If $E_0 < E$ the energy spectrum consists of two electron contours (curves 1) one of which disappears at $E_0 = E$ (curve 2). In larger fields the second contour splits into two contours (curves 3) at it was shown in Fig. 5a.

Figure 6 demonstrates the evolution of isoenergetic contour for the magnetic field directed along the axis $k_x = k_y$ (Sec. IVb). The disruption of the "neck" of the contour for the energy close to the saddle point $\epsilon_2^{sad}(h)$ (53) is shown in Fig. 6a: The contour 1 corresponds to $\epsilon_2^{sad}(h) < E$. The critical (self-crossing) contour 2 is in keeping with $\epsilon_2^{sad}(h) = E$. In higher fields the critical contour splits up into two disconnected parts (contours 3). Figure 6b demonstrates the appearance of self-crossing contour in the magnetic field at which $E_0(h) = E$.

In Fig. 7a, we have shown a possibility of specific changes in the topology by means of an in-plane rotation of the magnetic field in the case of equal SOI constants: the self-crossing contour (2) splits into two split-off contours (1,3) under a deflection of the magnetic field direction from symmetry axis $k_x = -k_y$. Figure 7b shows the splitting of self-crossing contour by the magnetic field for the energy close to minimal energy of branch contact points $\epsilon_{cont}^{\min}(0, h) = \hbar^2 h^2 / 8m\alpha^2$ (12).

VI. SINGULARITIES IN THE ELECTRON DENSITY OF STATES

Density of states (DOS) singularities are related to the critical points of energy spectrum. At the weak magnetic fields ($h < h_{c1}, h_{c2}$) results (26) and (28) obtained for 2D electrons with R-D SOI show that energies of both minima and saddle points move in opposite directions on the energy scale with the increasing of the value h . So, the number of van Hove's singularities is doubled by the magnetic field. Exclusions are the directions of vector \mathbf{h} along symmetry axes when two minima (47) ($\varphi_h = \pi/4, -3\pi/4$) or two saddle points (28) ($\varphi_h = 3\pi/4, -\pi/4$) "synchronously" move with a change in the magnetic field. In these cases the DOS has three singular points. At $h > h_{c1}$ the DOS contains two singularities which are associated with two minimum points at $h > h_{c2}$ or minimum and saddle points at $h < h_{c2}$.

By using the coordinates (13) the DOS can be found from the relations [38]

$$\rho(E) = \frac{m}{\pi\hbar^2}; \quad E \geq E_0, \quad (63)$$

$$\rho(E) = \frac{m}{2\pi^2\hbar^2} \sum_{j=1,2} \oint df \frac{\lambda^{(j)}}{\sqrt{\xi^{(j)}}} \Theta(\lambda^{(j)}) \Theta(\xi^{(j)}); E \leq E_0, \quad (64)$$

where $\lambda^{(j)}$ and $\xi^{(j)}$ are defined by Eqs. (15) and (60), $\Theta(x)$ is Heaviside step function. Equation (63) shows that the DOS is the same as for free 2D electron gas for energies $E \geq E_0$. When the opposite inequality $E < E_0$ the DOS $\rho(E)$ depends on the magnetic field and constants of SOI.

The electron density one find by integration of Eq.(64) over energies below Fermi level E_F [38]

$$n_e = \frac{m}{\pi\hbar^2} \left[E_F + \frac{m}{2\hbar^2} (\alpha^2 + \beta^2) \right] \quad (65)$$

for $E_F \geq E_0$.

The Van Hove singularities of $\rho(E)$ are related to minima and saddle points on the energy surfaces (58) and correspond to singularities in the integral (64) $\xi^{(j)}(f_{\nu}^{(j)}) = 0$. In order to separate the singular part of DOS near the critical point $E \rightarrow \epsilon_i^{crit}$, $f \rightarrow f_{\nu}^{(i)}$ we use a standard way. Equation (64) can be written as a sum of a convergent and divergent parts

$$\rho(E) = \rho_0(E) + \delta\rho(E), \quad (66)$$

$$\rho_0(E) = \frac{m}{2\pi^2\hbar^2} \sum_{j=1,2} \oint df \frac{\lambda^{(j)}(f) - \delta_{ij}\lambda^{(j)}(f_{\nu}^{(j)})}{\sqrt{\xi^{(j)}(f)}} \times \Theta(\lambda^{(j)}) \Theta(\xi^{(j)}), \quad (67)$$

$$\delta\rho(E) = \frac{m}{2\pi^2\hbar^2} \lambda^{(i)}(f_\nu^{(i)}) \oint \frac{df}{\sqrt{\xi^{(i)}(f)}} \Theta(\lambda^{(i)}) \Theta(\xi^{(i)}). \quad (69)$$

The continuous function $\xi^{(i)}(f)$ can be expanded as a Taylor series in a vicinity of the point $f = f_\nu^{(i)}$

$$\begin{aligned} \xi^{(1,2)}(f) &= \left(\lambda^{(1,2)}\right)^2 + \frac{2m(E - E_0)}{\hbar^2} \simeq \frac{2m(E - \epsilon_{1,2}^{crit})}{\hbar^2} \\ &+ \lambda^{(1,2)}(f_\nu^{(1,2)}) \ddot{\lambda}^{(1,2)}(f_\nu^{(1,2)}) (f - f_\nu^{(1,2)})^2 \\ &+ \frac{1}{6} \lambda^{(1,2)}(f_\nu^{(1,2)}) \lambda^{(1,2)}(f_\nu^{(1,2)}) (f - f_\nu^{(1,2)})^3 + \dots \end{aligned} \quad (70)$$

Substituting the expansion (70) into Eq. (69) we integrate using the cutoff of the integral by Θ -functions. At $E \rightarrow \epsilon_i^{crit}$ the singular term $\delta\rho(E)$ (69) does not depend on the interval of integration. As shown in Sec. III for the energy minima $\epsilon_{1,2}^{min}$ the second derivatives are negative, $\ddot{\lambda}^{(2)}(f_\nu^{(1,2)}) < 0$, and for the saddle points ϵ_2^{sad} the second derivatives are positive $\ddot{\lambda}^{(2)}(f_\nu^{(1,2)}) > 0$. As a result we have in a vicinity of the minimum points

$$\delta\rho(E) = \frac{m}{2\pi\hbar^2} \sqrt{\left| \frac{\lambda^{(1,2)}}{\ddot{\lambda}^{(1,2)}} \right|_{f=f_\nu^{(1,2)}}} \Theta(E - \epsilon_{1,2}^{min}). \quad (71)$$

For saddle point one finds

$$\begin{aligned} \delta\rho(E) &= -\frac{m}{2\pi^2\hbar^2} \sqrt{\frac{\lambda^{(2)}}{\ddot{\lambda}^{(2)}}} \\ &\times \ln \left[\frac{2m|E - \epsilon_2^{sad}|}{\hbar^2 \lambda^{(2)} \ddot{\lambda}^{(2)}} \right]_{f=f_\nu^{(2)}}. \end{aligned} \quad (72)$$

At the critical magnetic field $h = h_{c1}$ the first and second derivatives of $\lambda^{(2)}(f)$ are equal to zero, and the third term in the expansion (70) must be taken into account. The singular part of the DOS in the case of the degenerate critical point reads ($\ddot{\lambda}^{(2)} \neq 0$)

$$\begin{aligned} \delta\rho(E) &= \frac{m\sqrt{6}}{2\pi^{3/2}\hbar^2} \frac{\Gamma(\tau/6)}{\Gamma(2/3)} \\ &\times \sqrt{\left| \frac{\lambda^{(2)}}{\ddot{\lambda}^{(2)}} \right|_{f=f_\nu^{(2)}}} \left(\frac{12m|E - \epsilon_2^{crit}|}{\hbar^2 \lambda^{(2)} |\ddot{\lambda}^{(2)}|} \right)^{-1/6}. \end{aligned} \quad (73)$$

The results (71),(72) agree with the classical results for the two-dimensional case obtained in van Hove's paper [26]. The simple relations between the energies of critical points and SOI constants for directions of magnetic field along symmetry axes (see Sec.IV) is the way to find α and β from the position of DOS singularities on the magnetic field scale.

VII. CONCLUSIONS

The evolution of energy spectrum of 2D electron gas with combined Rashba and Dresselhaus SOI (3) under the influence of in-plane magnetic field \mathbf{B} has been analyzed for arbitrary SOI constants. It has been shown that geometry of energy surfaces (14) and isoenergetic contours (58) can be described by means of a single function (15), which depends on the magnetic field and SOI constants. We have found the relations which describe dependencies of critical point energies (25) and their positions (22) in the wave vector space on the vector \mathbf{B} . There are two critical values of magnetic field at which the essential transformation of the energy spectrum occurs: At the field $B = B_1$ (33) the minimum point and saddle point of the energy branch $\epsilon = \epsilon_2$ "annihilate" and at $B = B_2$ (32) the conical point of the branch $\epsilon = \epsilon_1$ transforms into the critical (minimum) point. Finally, the spectrum having four critical points (two minima and two saddle points) and a conical point at $B = 0$ evolves into spectrum with two minima at $B > B_1, B_2$. The general conclusions are illustrated for the directions of vector \mathbf{B} along the symmetry axes. On the basis of an analysis of spectrum critical points dependence on the magnetic field Lifshitz topological transitions in the geometry of isoenergetic contours have been studied (Figs.4-7). Along with critical contours related to spectrum critical points the appearance (or disappearance) of self - crossing contours with a magnetic field variation is found as well. Singular additions to the electron density of states have been derived (71) - (73). The positions of these singularities on the magnetic field scale make possible to find both the SOI constant. We have found $(-1/6)$ -root singularity for the degenerate critical points at $B = B_{c1}$ (73). The obtained results can be used for theoretical investigations of any kinetic and thermodynamic characteristics of 2D electrons with R-D SOI in the in-plane magnetic field as well as for interpretation of experimental data.

Magnetic-field-driven topological transitions can be observed in the 2D electron gas with a low electron density $n \simeq 10^9 \div 10^{10} \text{cm}^{-2}$ (see, for example, [39]). In heterostructures with higher density it could be essentially reduced by a negative gate voltage [40]. For the typical values of R-D SOI constants and an effective mass for $\text{Al}_x\text{Ga}_{1-x}\text{N}/\text{GaN}$ heterostructure, $\alpha \simeq 10^{-10} \text{eV} \cdot \text{cm}$, $\alpha/\beta \simeq 10$, $m = 0.2m_0$, $g^* = 2$ [41, 42] and $n \simeq 10^{10} \text{cm}^{-2}$, we estimate a Fermi energy, $E_F \simeq 0.1 \text{meV}$, by using Eq. (65). In this case the van Hove singularities appear in magnetic field $0 < B \lesssim 2T$. Other possibility to observe the predicted topological transitions is the in-plane tunnelling spectroscopy [43-45]. While a tunnelling conductances is proportional to the density of states at a shifted energy $\rho(\epsilon = E_F - eU)$, where eU is a bias energy, the electron states below Fermi level can be investigated.

ACKNOWLEDGMENTS

One of us (Yu.K) would like to acknowledge useful discussion with S. V. Kuplevakhsy.

Appendix: Functions $\lambda^{(1,2)}$ and $\ddot{\lambda}^{(1,2)}$ in the critical points of energy spectrum $\dot{\lambda}^{(1,2)} = 0$ for the magnetic field directed along symmetry axis.

Magnetic field directed along $k_x = -k_y$ axis

Substituting the angles (34),(35) corresponding to the zeros of $\dot{\lambda}^{(1,2)}$ we find the functions $\lambda^{(1,2)}$ (15)

$$\lambda^{(1,2)}\left(-\frac{3\pi}{4}\right) = \mp \frac{m}{\hbar^2}(\alpha + \beta) \mp \frac{h}{\alpha + \beta}, \quad (\text{A.1})$$

$$\lambda^{(1,2)}\left(\frac{\pi}{4}\right) = \mp \frac{m}{\hbar^2}(\alpha + \beta) \pm \frac{h}{\alpha + \beta}, \quad (\text{A.2})$$

$$\lambda^{(1,2)}(f_{3,4}) = \mp \frac{m}{\hbar^2}(\alpha - \beta) \sqrt{1 - \frac{h^2}{h_{c1}h_{c2}}}, \quad h \leq h_{c1}, \quad (\text{A.3})$$

and second derivatives $\ddot{\lambda}^{(1,2)}(f)$

$$\ddot{\lambda}^{(1,2)}\left(-\frac{3\pi}{4}\right) = \pm \frac{h + h_{c1}}{\alpha + \beta}, \quad (\text{A.4})$$

$$\ddot{\lambda}^{(1,2)}\left(\frac{\pi}{4}\right) = \mp \frac{h - h_{c1}}{\alpha + \beta}, \quad (\text{A.5})$$

$$\begin{aligned} \ddot{\lambda}^{(1,2)}(f_{3,4}) &= \mp \frac{h_{c1}}{\alpha - \beta} \left(1 - \left(\frac{h}{h_{c1}}\right)^2\right) \\ &\times \sqrt{1 - \frac{h^2}{h_{c1}h_{c2}}}; \quad h \leq h_{c1}. \end{aligned} \quad (\text{A.6})$$

The Eqs. (25), (A.1) - (A.3) give the formulas for energies which can be possible critical points $\epsilon^{crit \nu}(h) =$

$\epsilon_{1,2}\left(f_{\nu}^{(1,2)}\right)$ (25) of energy spectrum

$$\begin{aligned} \epsilon^{crit1}(h) &= -\frac{m}{2\hbar^2}(\alpha + \beta)^2 - h, \\ \epsilon^{crit2}(h) &= -\frac{m}{2\hbar^2}(\alpha + \beta)^2 + h, \end{aligned} \quad (\text{A.7})$$

$$\epsilon^{crit3,4}(h) = -\frac{m}{2\hbar^2}(\alpha - \beta)^2 + \frac{h^2\hbar^2}{8m\alpha\beta}. \quad (\text{A.8})$$

Magnetic field directed along $k_x = k_y$ axis.

The functions $\lambda^{(1,2)}$ in the points (44) of first derivatives $\dot{\lambda}^{(1,2)}$ zeros are given by

$$\lambda^{(1,2)}\left(\frac{3\pi}{4}\right) = \mp \frac{m}{\hbar^2}(\alpha - \beta) + \frac{h}{\alpha - \beta}, \quad (\text{A.9})$$

$$\lambda^{(1,2)}\left(-\frac{\pi}{4}\right) = \mp \frac{m}{\hbar^2}(\alpha - \beta) - \frac{h}{\alpha - \beta}, \quad (\text{A.10})$$

$$\lambda^{(1,2)}(f_{3,4}) = \mp \frac{m}{\hbar^2}(\alpha + \beta) \sqrt{1 + \frac{h^2}{h_{c1}h_{c2}}}, \quad h \leq h_{c1}, \quad (\text{A.11})$$

and their second derivatives $\ddot{\lambda}^{(1,2)}$ read

$$\ddot{\lambda}^{(1,2)}\left(\frac{3\pi}{4}\right) = -\frac{h - h_{c1}}{\alpha - \beta}, \quad (\text{A.12})$$

$$\ddot{\lambda}^{(1,2)}\left(-\frac{\pi}{4}\right) = \frac{h + h_{c1}}{\alpha - \beta}, \quad (\text{A.13})$$

$$\begin{aligned} \ddot{\lambda}^{(1,2)}(f_{3,4}) &= \pm \frac{h_{c1}}{\alpha + \beta} \left(1 - \left(\frac{h}{h_{c1}}\right)^2\right) \\ &\times \sqrt{1 + \frac{h^2}{h_{c1}h_{c2}}}; \quad h \leq h_{c1}. \end{aligned} \quad (\text{A.14})$$

As the last step one must separate the physical solutions: Only the positive values of $\lambda^{(1,2)}\left(f_{\nu}^{(1,2)}\right)$ satisfy to the Eq. (20). From the simple analysis of Eqs. (A.1)-(A.14) we obtain conditions of the extrema existence in different ranges of magnetic field.

-
- [1] I.M. Lifshitz, Sov. Phys. JETP, **11**, 1130 (1960).
[2] I.M. Lifshits, M.Ya. Azbel', and M.I. Kaganov, Electron Theory of Metals (Consultants Bureau, New York), (1973).
[3] A.A. Varlamov, V.S. Egorov, and A.V. Pantsulaya, Adv. Phys. **38**, 469 (1989).
[4] Ya.M. Blanter, M.I. Kaganov, A.V. Pantsulaya, A.A. Varlamov, Physics Reports **245**, 159-257 (1994).
[5] G.E. Volovik, Low Temp. Phys. **43**, 47 (2017); UFN, **188**, 95 (2018).
[6] A. Manchon, H. C. Koo, J. Nitta, S. M. Frolov and R. A. Duine, Nature Materials, **14**, 871 (2015).
[7] D. Bercioux, P. Lucignano, Report on Progress in Physics, **78** 106001 (2015).
[8] I.I. Boiko, E.I. Rashba. Sov. Phys. Solid State **2(8)**, 1692 (1961).
[9] G.A.H. Schober, H. Murakawa, M.S. Bahramy, R. Arita, Y. Kaneko, Y. Tokura, and N. Nagaosa, Phys. Rev. Lett. **108**, 247208 (2012).
[10] L. Meier, G. Salis, I. Shorubalko, E. Gini, S. Scho and K.

- Ensslin, Nature Physics, **3**, 650 (2007).
- [11] Y.F. Hao, Eur. Phys. J. B **85**: 84 (2012).
- [12] L. Silveira, P. Barone, and S. Picozzi, Phys. Rev. B **93**, 245159 (2016).
- [13] M. Kepenekian and J. Even, J. Phys. Chem. Lett., **8** (14), 3362 (2017).
- [14] S. D. Ganichev, and L. E. Golub, Phys. Status Solidi B **251**, 1801 (2014).
- [15] C.M. Wang Phys. Rev. B **82**, 165331 (2010).
- [16] M.A. Wilde and D. Grundler, New Journal of Physics **15** 115013 (2013).
- [17] D.H. Berman, M.E. Flatte, Phys. Rev. Lett. **105**, 157202 (2010).
- [18] S.M. Badalyan, A. Matos-Abiague, G. Vignale, and J. Fabian, Phys. Rev. B **81**, 205314 (2010).
- [19] I.V. Kozlov, Yu.A. Kolesnichenko, Low Temp. Phys. **43**, 855 (2017).
- [20] R. Winkler, Spin-Orbit Coupling Effects in Two-Dimensional Electron and Hole Systems (Springer-Verlag, Berlin Heidelberg, 2003).
- [21] Yu.V. Pershin, J.A. Nesteroff, and V. Privman, Phys. Rev. B **69**, 121306(R) (2004).
- [22] Yu.Ya. Tkach, JETP Letters **104**, 105 (2016).
- [23] O.N. Shevchenko and A.I. Kopeliovich, Low Temp. Phys., **42**, 196 (2016).
- [24] P.S. Alekseev, M.V. Yakunin and I. N. Yassievich, Semiconductors, **41**, 1092 (2007).
- [25] V. A. Sablikov and Yu. Ya. Tkach, Phys. Rev. B, **99**, 035436 (2019).
- [26] L. van Hove, Phys. Rev. **89**, 1189 (1953).
- [27] K. Wolff, R. Schafer, M. Meffert, D. Gerthsen, R. Schneider, and D. Fuchs, Phys. Rev. B, **95**, 245132 (2017).
- [28] R. Eppenga and M. F. H. Schuurmans, Phys. Rev. B, **37**, 10923 (1988).
- [29] A.M. Gilbertson, M. Fearn, J.H. Jefferson, B.N. Murdin, P.D. Buckle, and L.F. Cohen, Phys. Rev. B, **77**, 165335 (2008).
- [30] P. Kleinert, V.V. Bryksin, Phys. Rev. B, **76**, 205326 (2007).
- [31] C.M. Wang, Phys. Rev. B, **82** 165331 (2010).
- [32] Wen Xu , Yong Guo, Physics Letters A, **340** 281(2005).
- [33] E.I. Rashba, Sov. Phys. Solid State **2**, 1109 (1960), Yu. A. Bychkov, and E. I. Rashba, JETP Lett. **39**, 78 (1984).
- [34] G. Dresselhaus, Phys. Rev. **100**, 580 (1955).
- [35] Junsaku Nitta, Tatsushi Akazaki, and Hideaki Takayanagi, Phys. Rev. Lett. **78**, 1335 (1997).
- [36] Y. Sato, T. Kita, S. Gozu, and S. Yamada, J. Appl. Phys. **89**, 8017 (2001).
- [37] A.J.A. Beukman, F.K. de Vries, J. van Veen, etc., Phys. Rev. B **96**, 241401 (2017).
- [38] I.V. Kozlov, Yu.A. Kolesnichenko, arxiv.org. 1805.05699v1 (2018); Physics Letters A, **383**, 764 (2019).
- [39] J. Zhu, H.L. Stormer, L.N. Pfeiffer, K.W. Baldwin, and K.W. West, Phys. Rev. B. **90**, 056805 (2003).
- [40] C. Rossler, T. Feil, P. Mensch, T. Ihn, K. Ensslin, D. Schuh, and W. Wegscheider, New Journal of Physics **12** 043007 (2010).
- [41] Chunming Yin, Bo Shen, Qi Zhang, Fujun Xu, Ning Tang, Longbin Cen, Xinqiang Wang, Yonghai Chen, and Jinling Yu, Applied Phys. Lett. **97**, 181904 (2010).
- [42] W. Knap, E. Frayssinet, and M.L. Sadowski, C. Skierbiszewski, D. Maude, V. Falko, M. Asif Khan, M. Asif Khan, Applied Phys. Lett. **75**, 3156 (1999).
- [43] Yee Sin Ang, Zhongshui Ma and C. Zhang, Scientific Reports **4**, 3780 (2014).
- [44] B. Srisongmuang, P. Pairor, Phys. Rev. B. **78**, 155317 (2008).
- [45] A. Jantayod, P. Pairor, Physica E, **48**, 111 (2013).